Two-dimensional resonance enhanced multiphoton ionization of H^{i}Cl; $i = 35, 37$: State interactions, photofragmentations and energetics of high energy Rydberg states

Kristján Matthíasson, Jingming Long, Huasheng Wang, and Ágúst Kvaran[a)]
Science Institute, University of Iceland, Dunhagi 3, 107 Reykjavík, Iceland

(Received 8 February 2011; accepted 5 March 2011; published online 22 April 2011)

Mass spectra were recorded for $(2 + n)$ resonance enhanced multiphoton ionization (REMPI) of HCl as a function of resonance excitation energy in the 88865-89285 cm^{-1} region to obtain two-dimensional REMPI data. Band spectra due to two-photon resonance transitions to number of Rydberg states ($\Omega' = 0$, 1, and 2) and the ion-pair state $V(^1\Sigma^+(\Omega' = 0))$ for $H^{35}Cl$ and $H^{37}Cl$ were identified, assigned, and analyzed with respect to Rydberg to ion-pair interactions. Perturbations show as line-, hence energy level-, shifts, as well as ion signal intensity variations with rotational quantum numbers, J', which, together, allowed determination of parameters relevant to the nature and strength of the state interactions as well as dissociation and ionization processes. Whereas near-resonance, level-to-level, interactions are found to be dominant in heterogeneous state interactions ($\Delta\Omega \neq 0$) significant off-resonance interactions are observed in homogeneous interactions ($\Delta\Omega = 0$). The alterations in Cl^+ and HCl^+ signal intensities prove to be very useful for spectra assignments. Data relevant to excitations to the $j^3\Sigma(0^+)$ Rydberg states and comparison with $(3 + n)$ REMPI spectra allowed reassignment of corresponding spectra peaks. A band previously assigned to an $\Omega = 0$ Rydberg state was reassigned to an $\Omega = 2$ state ($\nu^0 = 88957.6$ cm^{-1}). © *2011 American Institute of Physics*. [doi:10.1063/1.3580876]

I. INTRODUCTION

Since the original work by Price on the hydrogen halides,[1] a wealth of spectroscopic data on HCl has been derived from absorption spectroscopy,[2–5] fluorescence studies[5] as well as from resonance enhanced multiphoton ionization (REMPI) experiments.[6–20] Relatively intense single- and multiphoton absorption in conjunction with electron excitations as well as rich band structured spectra make the molecule ideal for fundamental studies. A large number of Rydberg states, several low-lying repulsive states as well as the $V(^1\Sigma^+)$ ion-pair state have been identified. A number of spin-forbidden transitions are observed, indicating that spin–orbit coupling is important in excited states of the molecule. Perturbations due to state mixing are widely seen both in absorption[3–5] and REMPI spectra.[7,8,10,12,13,15,16,20] The perturbations appear either as line shifts[4,7,8,10,13,15,16,20] or as intensity and/or bandwidth alterations.[4,7,8,10,12,13,15,16,20] Pronounced ion-pair to Rydberg state mixings are both observed experimentally[3,4,8,10,13,15,16,20,21] and predicted from theory.[21,22] Interactions between the $V(^1\Sigma^+)$ ion-pair state and the $E(^1\Sigma^+)$ state are found to be particularly strong and to exhibit nontrivial rotational, vibrational, and electron spectroscopy due to a production of a mixed (adiabatic) $B^1\Sigma^+$ state with two minima. Perturbations due to Rydberg–Rydberg mixings have also been predicted and identified.[4,12] Both homogeneous ($\Delta\Omega = 0$)[15,16,21,22] and heterogeneous ($\Delta\Omega \neq 0$)[16,20,21] couplings have been reported. Such quantitative data on molecule–photon interactions are of interest in understanding stratospheric photochemistry as well as being relevant to the photochemistry of planetary atmospheres and the interstellar medium.[5]

Photofragment studies of HCl have revealed a large variety of photodissociation and photoionization processes. In a detailed two-photon resonance enhanced multiphoton ionization study, Green *et al.* report HCl^+, Cl^+, and H^+ ion formations for excitations via large number of $\Omega = 0$ Rydberg states as well as via the $V^1\Sigma^+$ ($\Omega = 0$) ion-pair state, whereas excitations via other Rydberg states are mostly found to yield HCl^+ ions.[7] More detailed investigations of excitations via various Rydberg states and the $V^1\Sigma^+$ ion-pair state by use of photofragment imaging and/or mass-resolved REMPI techniques have revealed several ionization channels depending on the nature of the resonance excited state.[23–30] The number of REMPI studies performed by our group for resonance excitations to the $F^1\Delta_2$ Rydberg state[16,27] and several triplet Rydberg states[16,27] as well as the $V^1\Sigma^+$ ion-pair states have revealed near-resonance interactions between the Rydberg and the ion-pair states. This shows as relative ion signal alterations in all cases[27,28,30] and/or as line shifts in all cases except for the weakest interactions.[16,20,29] Data analysis has allowed determination of interaction strength. The resonance interpretation has been confirmed by proton formation studies for REMPI via the $F^1\Delta_2$ ($v' = 1$, $J' = 8$) and $f^3\Delta_2(v' = 0$, $J' = 2$–$6)$ Rydberg states using three-dimensional velocity mapping.[29] All in all REMPI photofragmentation studies of HCl have revealed characteristic ionization channels which have been summarized in terms of excitations via (1)

[a)]Author to whom correspondence should be addressed. Electronic mail: agust@hi.is. Permanent address: Science Institute, University of Iceland, Dunhagi 3, 107 Reykjavík, Iceland, Tel: +354-525-4672/4800, Fax: +354-552-8911.

excitations via resonance noncoupled (diabatic) Rydberg state excitations, (2) excitations via resonance noncoupled (diabatic) ion-pair excitations, and (3) dissociation channels involving dissociation and/or photodissociation of resonance excited Rydberg states.[28]

In this paper, we use a two-dimensional (2D) REMPI data, obtained by recording ion mass spectra as a function of laser frequency, to study the state interactions and photofragmentation dynamics of HCl following two-photon resonance excitations to the triplet Rydberg states $j^3\Sigma\ (0^+)\ (v' = 0)$, $j^3\Sigma^-_1\ (v' = 0)$, the $V^1\Sigma^+\ (v' = 20, 21)$ ion-pair states as well as to Rydberg states, named *A* and *B* here, which band origins are at $\nu^0 = 88948.4\ \text{cm}^{-1}$ $\nu^0 = 88959.9\ \text{cm}^{-1}$, respectively, according to Green *et al.*[9] Rotational line shifts and quantum level dependent ion signal intensities, due to perturbation effects, are observed for the $H^{35}Cl$ and/or $H^{37}Cl$ isotopomers. By a combined analysis of the line shifts and signal intensities, interaction strengths, fractional state mixings, and parameters relevant to dissociation and ionization processes were evaluated. The perturbation observations as well as comparison of $(2 + n)$ and $(3 + n)$ REMPI data proved to be very helpful for assigning spectra bands. Lines due to transitions to the $j^3\Sigma\ (0^+)\ (v' = 0)$ and the *A* states were reassigned. The $\nu^0 = 88948.4\ \text{cm}^{-1}$ band, previously assigned to an $\Omega = 0$ state was reassigned to an $\Omega = 2$ state.

II. EXPERIMENTAL

Two-dimensional REMPI data for jet cooled HCl gas were recorded. Ions were directed into a time-of-flight tube and detected by a microchannel plate (MCP) detector to record the ion yield as a function of mass and laser radiation wavenumber. The apparatus used is similar to that described elsewhere.[19,30,31] Tunable excitation radiation in the 224.0–225.0 nm wavelength region was generated by an Excimer laser-pumped dye laser system, using a Lambda Physik COMPex 205 Excimer laser and a Coherent ScanMatePro dye laser. The dye C-440 was used and frequency doubling obtained with a BBO-2 crystal. The repetition rate was typically 10 Hz. The bandwidth of the dye laser beam was about $0.095\ \text{cm}^{-1}$. Typical laser intensity used was 0.1–0.3 mJ/pulse. The radiation was focused into an ionization chamber between a repeller and an extractor plate. We operated the jet in conditions that limited cooling in order not to lose transitions from high rotational levels. Thus, an undiluted, pure HCl gas sample (Merck-Schuchardt OHG; purity >99.5%) was used. It was pumped through a 500 μm pulsed nozzle from a typical total backing pressure of about 2.0–2.5 bar into the ionization chamber. The pressure in the ionization chamber was lower than 10^{-6} mbar during experiments. The nozzle was kept open for about 200 μs and the laser beam was typically fired 500 μs after opening the nozzle. Ions were extracted into a time-of-flight tube and focused onto a MCP detector, of which the signal was fed into a LeCroy 9310 A, 400 MHz storage oscilloscope and/or a LeCroy WaveSurfer 44MXs-A, 400 MHz storage oscilloscope as a function of flight time. Average signal levels were evaluated and recorded for a fixed number of laser pulses (typically 100 pulses) to obtain the mass spectra. Mass spectra were typically recorded in 0.05 or $0.1\ \text{cm}^{-1}$ laser wavenumber steps to obtain 2D REMPI spectra. REMPI spectra for certain ions as a function of excitation wavenumber (1D REMPI) were obtained by integrating mass signal intensities for the particular ion. Care was taken to prevent saturation effects as well as power broadening by minimizing laser power. Laser calibration was performed by recording an optogalvanic spectrum, obtained from a built-in Neon cell, simultaneously with the recording of the REMPI spectra. Line positions were also compared with the strongest hydrogen chloride rotational lines reported by Green *et al.*[9] The accuracy of the calibration was found to be about $\pm 1.0\ \text{cm}^{-1}$ on a two-photon wavenumber scale. Intensity drifts during the scan were taken into account, and spectral intensities were corrected accordingly. Experimental conditions for the three-photon excitation are described in Ref. 20.

III. RESULTS AND ANALYSIS

A. REMPI spectra and relative ion signals for the $j^3\Sigma^-_1 \leftarrow\leftarrow X^1\Sigma^+$ (0, 0) transitions

Figure 1 shows 2D-REMPI contour (below) and corresponding 1D-REMPI spectra (above) for the narrow spectral region of 88990–89080 cm^{-1}. The figure shows *Q* lines

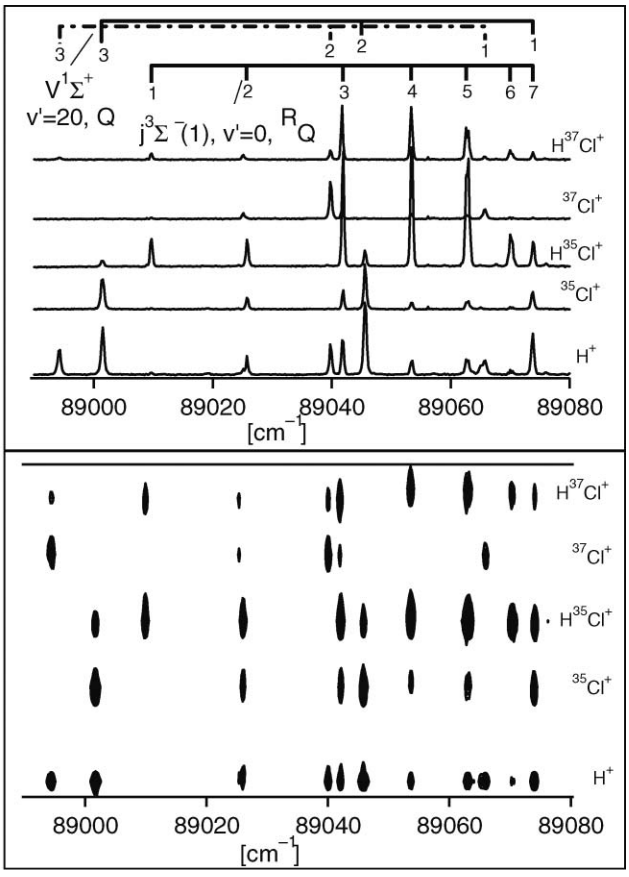

FIG. 1. 2D-$(2 + n)$ REMPI spectra (below) and corresponding 1D REMPI spectra (above) for H^+, $^{35}Cl^+$, $H^{35}Cl^+$, $^{37}Cl^+$, and $H^{37}Cl^+$ derived from HCl with isotope ratios in natural abundance for the two-photon excitation region of 88990– 89080 cm^{-1}. Assignments for the *Q* line series of the $j^3\Sigma_1 \leftarrow\leftarrow X^1\Sigma^+$ (0, 0) ($H^{35}Cl$ and $H^{37}Cl$: solid lines) and $V^1\Sigma^+ \leftarrow\leftarrow X^1\Sigma^+$ (20, 0) ($H^{35}Cl$: solid lines; $H^{37}Cl$: broken lines) spectra are shown. $J = J'$—numbers are indicated in the figure.

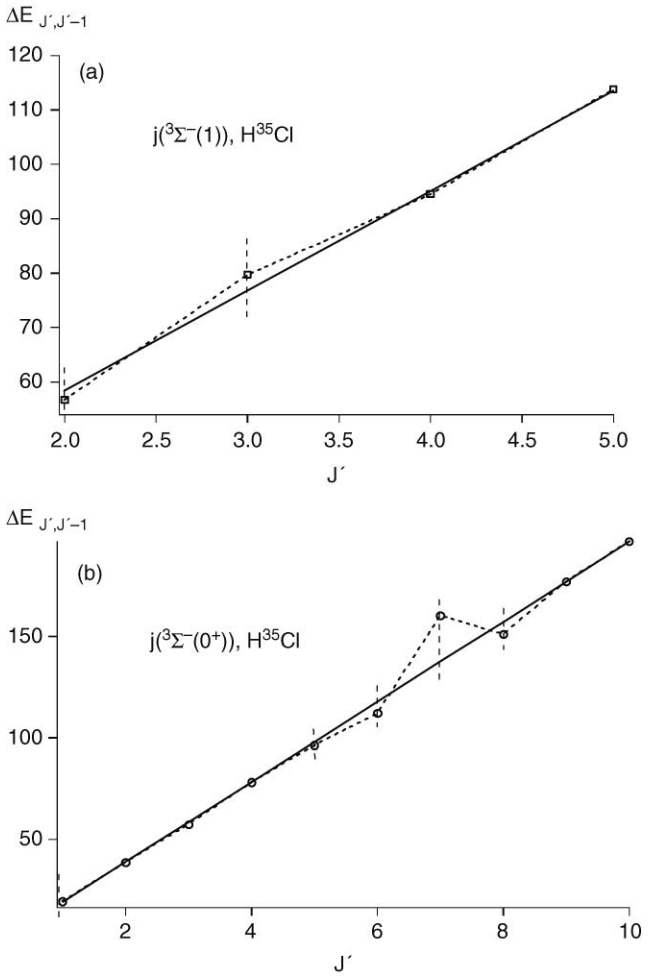

FIG. 2. $H^{35}Cl$: Spacings between rotational levels ($\Delta E_{J',J'-1}$) as a function of J' for the $j^3\Sigma^-(1)$ (a) and $j^3\Sigma^-(0^+)$ (b) Rydberg states for $H^{35}Cl$ derived from Q rotational lines.

due to the transitions $j^3\Sigma^-_1 \leftarrow\leftarrow X^1\Sigma^+$ (0, 0) and $V^1\Sigma^+ \leftarrow\leftarrow X^1\Sigma^+$ (20, 0), for the $H^{35}Cl$ and $H^{37}Cl$ isotopomers and their ion fragments.

Small but significant shift of peaks due to transitions to $J' = 2$ and 3 levels is observed. This shows as deviation in energy level spacings ($\Delta E_{J',J'-1} = E(J')-E(J'-1)$) from linearity for the corresponding rotational energy levels ($E(J')$) derived from measured peak positions and known rotational energy levels for the ground electronic state [see Fig. 2(a)]. This is a characteristic for a near-resonance level-to-level rotational interaction between the Rydberg state (1) and the $V(^1\Sigma^+)$ ion-pair state (2).[16,20] The smallest spacing between rotational energy levels of the two states for the same J' quantum numbers ($\Delta E_{J'} = E_1(J')–E_2(J')$) is found to be for $J' = 2$ and 3 for the $V(v' = 20)$ state (see Table I). First order unshifted energy levels, both for the $j^3\Sigma^-_1$ (1) and the $V(^1S^+)$ (2) states, $E_1{}^0(J')$ and $E_2{}^0(J')$, respectively, were derived from the linear fits for $\Delta E_{J',J'-1}$ versus J' [see Fig. 2(a)] and the energy level values for unshifted levels. From these and energies of perturbed levels ($E(J')$) interaction strengths (W_{12}) could be derived as a function of J' from

$$W_{12}(J') = \left[\frac{1}{4}\left\{\left(2\left(\left\langle\frac{1}{2}\left(E_1^0(J')+E_2^0(J')\right)\right\rangle - E_1(J')\right)\right)^2 - \left(E_1^0(J')-E_2^0(J')\right)^2\right\}\right]^{1/2}. \quad (1)$$

The interaction strength parameter, W'_{12} was derived from the expression $W_{12}(J') = W'_{12}\,(J'(J'+1))^{1/2}$ which holds for a heterogeneous interaction ($\Delta\Omega \neq 0$) (see Table II). The fractional contributions to the state mixing [c_1^2 for the Rydberg state (1) and c_2^2 for the ion-pair state (2)] are now easily derived from W_{12} and the energy difference $\Delta E_{J'} = E_1(J') - E_2(J')$ as

$$c_1^2 = \frac{1}{2} + \frac{\sqrt{(\Delta E_{J'})^2 - 4\,(W_{12})^2}}{2\,|\Delta E_{J'}|}; \quad c_2^2 = 1 - c_1^2. \quad (2)$$

Significant enhancement of the relative Cl^+ signals ($I(^{35}Cl^+)/I(H^{35}Cl^+)$) and $I(^{37}Cl^+)/I(H^{37}Cl^+)$) is observed for $j^3\Sigma^-_1 \leftarrow\leftarrow X^1\Sigma^+$, (0, 0), Q lines, $J' = 2$ [see Figs. 3(a) and 3(b)] also characteristic for the near-resonance interaction.[16,20,27] The $H^{37}Cl$ isotopomer shows considerably larger intensity ratio than the $H^{35}Cl$ isotopomer. An expression for $I(Cl^+)/I(HCl^+)$ as a function of the mixing fraction, c_2^2, based on ionization processes following resonance excitation, has been derived,[28]

$$\frac{I(Cl^+)}{I(HCl^+)} = \frac{\alpha\left[\gamma + c_2^2(1-\gamma)\right]}{\left(1-c_2^2\right)}, \quad (3)$$

$$I(Cl^+) = \alpha_2 c_2^2 + \beta_1 c_1^2; \quad I(HCl^+) = \alpha_1 c_1^2 + \beta_2 c_2^2$$

TABLE I. $\Delta E_{J'}$ relevant to near-resonance interactions for $j^3\Sigma^-_1 \leftrightarrow V^1\Sigma^+, v' = 20$, $j^3\Sigma^-(0^+) \leftrightarrow V^1\Sigma^+, v' = 20$, 21, State $A \leftrightarrow V^1\Sigma^+, v' = 20$, and State $B \leftrightarrow V^1\Sigma^+, v' = 20$.

	$\Delta E_{j'} = E(j^3\Sigma^-_1; v'=0) - E(V^1\Sigma^+; v'=20)$		$\Delta E_{j'} = E(j^3\Sigma^-(0^+); v'=0) - E(V^1\Sigma^+; v'=20/21)$		$\Delta E_{j'} = E$(State A) $-E(V^1\Sigma^+; v'=20)$	$\Delta E_{j'} = E$(State B) $-E(V^1\Sigma^+; v'=20)$
J'	$H^{35}Cl$	$H^{37}Cl$	$H^{35}Cl$ ($v'=20/21$)	$H^{37}Cl$ ($v'=20/21$)	$H^{35}Cl$	$H^{35}Cl$
0			196.4/−304.3	214.8/–316.1		
1	− 62.2	− 55.7	208.9/−311.6	215,4/–305.7		
2	− 20.6	− 14.7	232.4/−284.2	238.2/–280.6	− 96.6	− 92.7
3	40.2	47.9	271.6/−245.1	278.9/–241.7	− 62.0	− 59.3
4	108.2	115.1	322.5/−193.8	328.9/–190.4	− 22.0	− 13.8
5	187.3	192.1	384.2/−129.6	394.0/–130.7	26.0	45.4
6	279.0		457.4/–71	462.6/–65	88.0	117.2

TABLE II. Parameter values, relevant to state mixing, derived from peak shifts and intensity ratios ($I(^iCl^+)/I(H^iCl^+)$) as a function of J'. See definitions of parameters in the text.

	$j^3\Sigma^-{}_1$; $v'=0$		$j^3\Sigma^-(0^+)$; $v'=0$		State B
Isotopomers	$H^{35}Cl$	$H^{37}Cl$	$H^{35}Cl$	$H^{37}Cl$	$H^{35}Cl$
J' closest resonances (J'_{res})	2	2	7(6)	6(7)	4
$\lvert\Delta E(J'_{res})\rvert(cm^{-1})$	20.6	14.7	? (71)[a,b]	65(?)[a,b]	13.8
$W_{12}(cm^{-1})$	6.5	5.8	25	25	2.7
$W'_{12}(cm^{-1})$	2.7	2.4	...	...	0.6
$c_1^2(c_2^2)$	0.89(0.11)	0.81(0.19)	0.88(0.12)	0.82(0.18)	0.96(0.04)
γ	0.004	0.003	(0.031)[c]	0.013	0.002
α	3.5	4.2	(2.1)[c]	4.0	3.1

[a]Values for $J'=7$ could not be determined since rotational peaks due to transitions to $V(v'=21, J'=7)$ were not observed.
[b]Values for $J'=6$ were derived from observations of weak and broad rotational lines in the Q series due to transitions to $V(v'=21, J'=6)$ at 89317.4 cm^{-1} and 89311.1 cm^{-1} for $H^{35}Cl$ and $H^{37}Cl$, respectively.
[c]Parameters are uncertain due to overlap of spectra peaks for transitions to $J'=6$ and 8. The γ value is an upper limit value. The α value is a lower limit value.

where $\alpha(=\alpha_2/\alpha_1)$ measures the relative rate of the two major/characteristic ionization channels, i.e., for the Cl^+ formation for excitation from the diabatic ion-pair state (α_2) to the HCl^+ formation from the diabatic Rydberg state (α_1). Here, γ ($=\beta_1/\alpha_2$) represents the rate of Cl^+ formation via the diabatic Rydberg state (β_1; referred to as the "dissociative channel" in Ref. 28) to that of its formation from the diabatic ion-pair state (α_2), which is one of the major/characteristic ionization channels. Hence, γ is a relative measure of the importance of the "dissociative channel." Expression (3) allows the relative ion signals as a function of J' to be fitted to derive α and γ [Figs. 3(a) and 3(b) and Table II]. The larger Cl^+

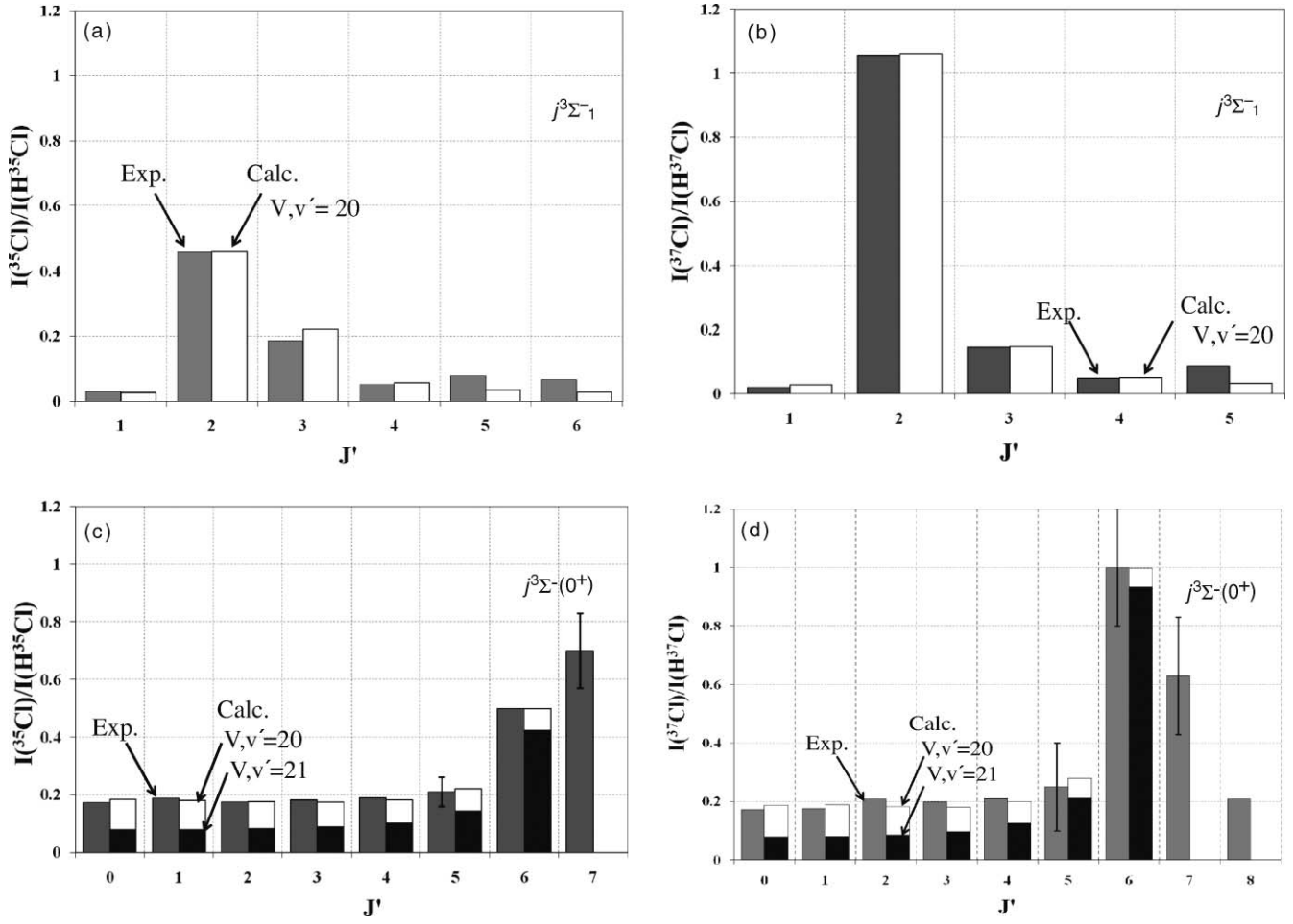

FIG. 3. Relative ion signal intensities, $I(^iCl^+)/I(H^iCl^+)$ ($i=35$ and 37) vs J' derived from Q rotational lines of REMPI spectra due to resonance transitions to Rydberg states (gray columns) and simulations, assuming J' level-to-level interactions between the Rydberg states and the $V^1\Sigma^+$ ($v'=20, 21$) states (white and black columns): (a) $H^{35}Cl$, $j^3\Sigma^-{}_1 \leftrightarrow V^1\Sigma^+$ ($v'=20$) interactions, (b) $H^{37}Cl$, $j^3\Sigma^-{}_1 \leftrightarrow V^1\Sigma^+$ ($v'=20$) interactions, (c) $H^{35}Cl$, $j^3\Sigma^-(0^+) \leftrightarrow V^1\Sigma^+$ [$v'=20$ (white columns) and $v'=21$ (black columns)] interactions, and (d) $H^{37}Cl$, $j^3\Sigma^-(0^+) \leftrightarrow V^1\Sigma^+$ [$v'=20$ (white columns) and $v'=21$ (black columns)] interactions.

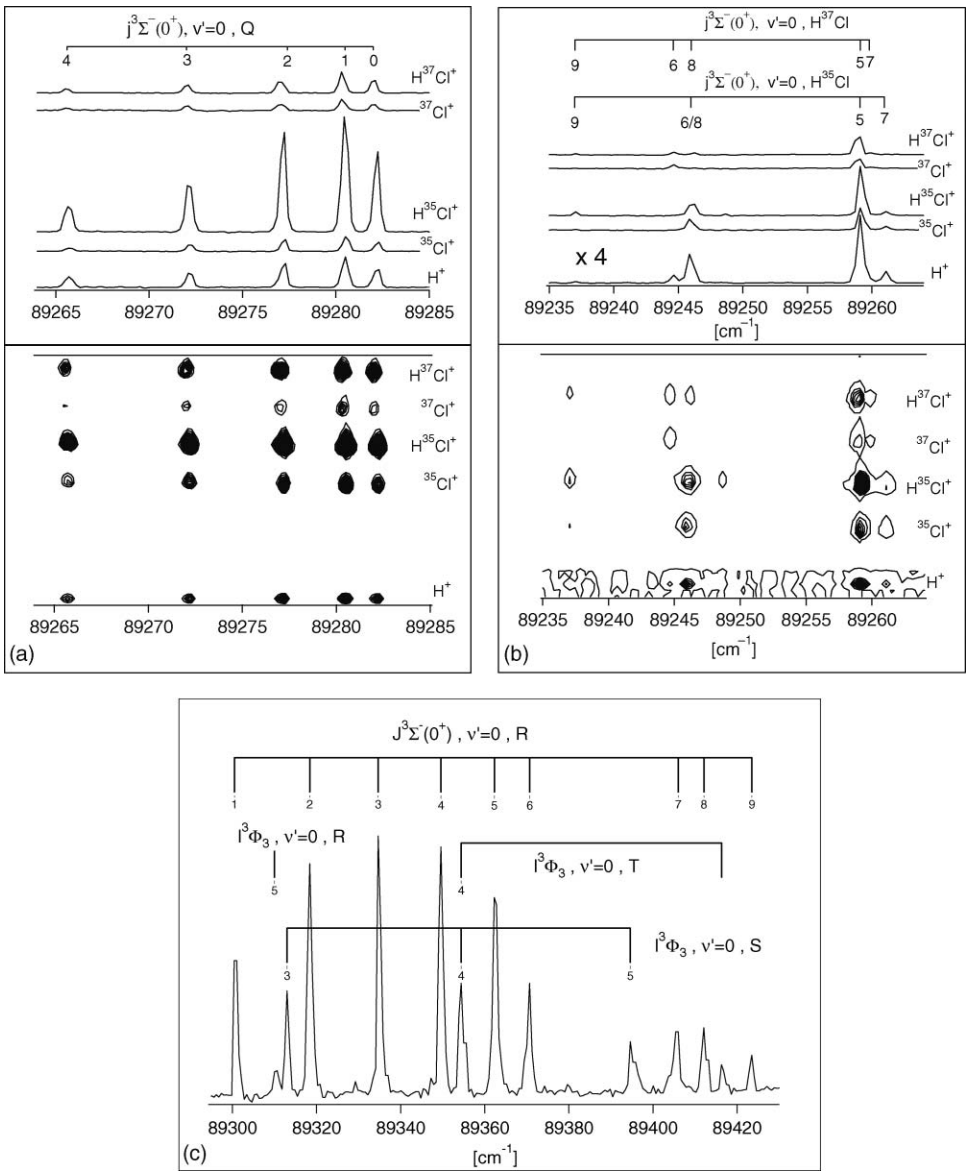

FIG. 4. (a) and (b) 2D-(2 + *n*) REMPI spectra (below) and corresponding 1D REMPI spectra (above) for H^+, $^{35}Cl^+$, $H^{35}Cl^+$, $^{37}Cl^+$, and $H^{37}Cl^+$ derived from HCl with isotope ratios in natural abundance for the two-photon excitation regions of 89264–89285 cm^{-1} (a) and 89235–89265 cm^{-1} (b). Assignments for the *Q* line series of the $j^3\Sigma^-(0^+) \leftarrow\leftarrow X^1\Sigma^+$ (0, 0) ($H^{35}Cl$ and $H^{37}Cl$) spectra are shown. The intensities of the 1D REMPI spectra in the 89235 –89265 cm^{-1} spectral region (b) have been multiplied by factor 4 with respect to the corresponding intensities in 89264–89285 cm^{-1} spectral region (a). (c) 1D-(3 + n) REMPI spectrum for total ionization of HCl for the three-photon excitation region of 89295–89430 cm^{-1}. Assignments for the $j^3\Sigma^-(0^+) \leftarrow\leftarrow X^1\Sigma^+$ (0, 0) and $l^3\Phi_3 \leftarrow\leftarrow X^1\Sigma^+$ (0, 0) transitions ($H^{35}Cl$ and $H^{37}Cl$) are shown. $J = J'$—numbers are indicated in the figures.

fragmentation observed for $H^{37}Cl$ compared to that for $H^{35}Cl$ can be understood by comparison of the derived parameters listed in Table II. Whereas the interaction strengths are comparable, for the two isotopomers the ion-pair mixing fraction (c_2^2) is significantly larger for $H^{37}Cl$ ($c_2^2 = 0.19$) than for $H^{35}Cl$ ($c_2^2 = 0.11$). This is primarily due to the smaller energy gap ($\Delta E_{J'} = 14.7$ cm^{-1}) between the mixing rotational states for $H^{37}Cl$ compared to that for $H^{35}Cl$ ($\Delta E_{J'} = 20.6$ cm^{-1}). The gamma values (γ) obtained, both for the $H^{35}Cl$ ($\gamma = 0.004$) and the $H^{37}Cl$ ($\gamma = 0.003$) isotopomers are small values and comparable to those obtained before for the triplet states $f^3\Delta_1$ and $g^3\Sigma^+$[28,30] indicating a small, but non-negligible contribution of the dissociation channels to the Cl^+ signal. Judging from a coupling scheme given by Alexander *et al.*[32] this could be formed after a direct predissociation of the $j^3\Sigma^-_1$ state by spin–orbit coupling with the repulsive $t^3\Sigma^+_1$ state and/or after predissociation of nearby Rydberg states ($^1\Pi$, $^3\Pi_2$) which could act as gateways via S/O coupling with the $j^3\Sigma^-_1$ states.

B. REMPI spectra and relative ion signals for the $j^3\Sigma^-(0^+) \leftarrow\leftarrow X^1\Sigma^+$ (0, 0) transitions

Figures 4(a) and 4(b) show 2D and 1D (2 + *n*) REMPI spectra for the narrow excitation region of 89235–89285 cm^{-1}. The figures show the *Q* lines due to the $j^3\Sigma^-(0^+) \leftarrow\leftarrow X^1\Sigma^+$ (0, 0) resonance transitions for $H^{35}Cl$ and $H^{37}Cl$. Total 1D (3 + *n*) REMPI spectrum is shown in Fig. 4(c) for the spectral region 89300–89430 cm^{-1}. It shows *R* lines for

TABLE III. Rotational lines for the $j^3\Sigma^-(0^+) \leftarrow\leftarrow X^1\Sigma^+$ (0, 0) transitions (HCl). The line positions are common to $H^{35}Cl$ and $H^{37}Cl$ except for the Q lines, $J' = 6$ and 7, in which case the values for $H^{37}Cl$ are inside brackets.

	$j^3\Sigma^-(0^+) \leftarrow\leftarrow X^1\Sigma^+$ (0, 0)		
J'	O	Q	S
0	89219.6	89282.0	
1	89176.2	89280.5	
2	89131.4	89277.3	89340.1
3		89272.1	89377.3
4		89266.8	89412.8
5		89259.0	89446.7
6		89246.3	89475.9
		(89244.7)	
7		89261.1	
		(89259.9)	
8		89246.3	
9		89237.1	

the same electronic transitions as well as peaks due to transitions to the $l^3\Phi_3$ state.[20] Clear gap between the $J' = 6$ and $J' = 7$ rotational lines is observed for the R lines. This gap corresponds to the smallest spacing between observed rotational energy levels for the $j^3\Sigma^-(0^+)$ ($v' = 0$) and rotational energy levels for the $V^1\Sigma^+$ ($v' = 21$) states for equal J' values (see Table I) suggesting a near-resonance interaction between the two states.[16,20,27] Comparison of peak positions in $(3 + n)$ and $(2 + n)$ REMPI spectra and relative intensities of ion peaks, allowed assignment of the Q line rotational peaks both for $H^{35}Cl$ and $H^{37}Cl$ in the $(2 + n)$ REMPI spectrum. Irregular arrangement of peaks, with respect to J' numbering, is seen for $J' = 5$–9 [see Fig. 4(b)] and enhanced intensity ratios ($I(^iCl^+)/I(H^iCl^+)$) are observed for transitions to $J' = 6$ and 7 [Figs. 3(c) and 3(d)]. See also Table III. Peak assignments differ from earlier assignments.[9,20]

Analogous and relatively large deviation in energy level spacings ($\Delta E_{J',J'-1}$) from linearity is clearly seen both for $H^{35}Cl$ and $H^{37}Cl$ [see Fig. 2(b)]. This allowed the interaction strengths (W_{12}) to be evaluated for $J' = 5$–8 analogous to that described before. A relatively large interaction strength value of about 25 ± 3 cm^{-1} was obtained both for $H^{35}Cl$ and $H^{37}Cl$ independent of J' as to be expected for homogeneous interactions (Table II). Despite difference in line assignments this value is comparable to that reported earlier in Ref. 20 ($W_{12} = 20 \pm 4$ cm^{-1}). The large homogeneous interaction strength results in off-resonance interactions between J' states showing as significant mixing contribution for the ion-pair state (c_2^2) over a wide range of J' states, both for $V(v' = 20)$ and $V(v' = 21)$. This results in significant contributions to the ion ratios from off-resonance interactions according to Eq. (3). Mixing contributions from vibrational states further away in energy ($v' < 20$ and $v' > 21$), on the other hand, are negligible, assuming the interaction strength (W_{12}) to be comparable.

Assuming, to a first approximation, that the ion intensity ratio is a sum of contributions due to interactions from the $V(v' = 20)$ and $V(v' = 21)$ states for common α and γ parameters $I(^{37}Cl^+)/I(H^{37}Cl^+)$ can be expressed as

$$\frac{I(Cl^+)}{I(HCl^+)} = \alpha \left\{ \frac{\left[\gamma + c_{2,20}^2(1-\gamma)\right]}{\left(1 - c_{2,20}^2\right)} + \frac{\left[\gamma + c_{2,21}^2(1-\gamma)\right]}{\left(1 - c_{2,21}^2\right)} \right\}, \quad (4)$$

where $c_{2,20}^2$ and $c_{2,21}^2$ are the fractional mixing contributions for $V(v' = 20)$ and $V(v' = 21)$, respectively. Figure 3(d) shows least square fit of the data for $I(^{37}Cl^+)/I(H^{37}Cl^+)$ versus J' as well as the $V(v' = 20)$ and $V(v' = 21)$ contributions for the α and γ parameters listed in Table II. The calculations are limited to $J' < 7$ since rotational lines for higher J', hence energy levels, for $V(v' = 21)$ could not be observed. Due to uncertainty in the ion-ratio value for $J' = 6$ because of overlap of Q line peaks for $J' = 6$ and 8 analogous least square analyses could not be performed for $H^{35}Cl$ [Fig. 3(c)]. The characteristic large and J'-independent ion intensity ratios for $J' < 5$, observed both for $H^{35}Cl$ and $H^{37}Cl$ result in a relatively large γ factor, an order of magnitude bigger than those determined for other triplet states, $\Omega' > 0$ mentioned before. This suggests that the "dissociation channels" are of greater importance. As mentioned before the small contributions to the dissociation channels for the other triplet states has been interpreted as being due to predissociation via gateway states.[28] Based on the coupling schemes given by Alexander *et al.*[32] such channels for the $j^3\Sigma^-$ states are limited. The "enhanced" importance of "dissociation channels" therefore could be due to an opening of a dissociation channel via photoexcitation to an inner wall of a bound excited Rydberg state above the dissociation limit.[28]

C. REMPI spectra and relative ion signals for the $A \leftarrow\leftarrow X^1\Sigma^+$ (0, 0) and $B \leftarrow\leftarrow X^1\Sigma^+$ (0, 0) transitions

Figure 5 shows 1D-REMPI spectra for the narrow spectral region of 88865–88985 cm^{-1}. The figure shows the Q lines due to the transitions $A \leftarrow\leftarrow X\ ^1\Sigma^+$ (0, 0) and $B \leftarrow\leftarrow X\ ^1\Sigma^+$ (0, 0) both for the $H^{35}Cl^+$ and $H^{37}Cl^+$ ions and corresponding ion fragments. Also it shows rotational lines due to the transitions $j^3\Sigma^-_1 \leftarrow\leftarrow X^1\Sigma^+$ (0, 0), $\Omega \leq 2 \leftarrow\leftarrow X^1\Sigma^+$ (0, 0), and $V^1\Sigma^+ \leftarrow\leftarrow X^1\Sigma^+$ (20, 0).

Slight but significant enhancement in spacing between rotational levels $J' = 5$ and 4 is observed for the B state and clear increase in the relative $^{35}Cl^+$ signal intensity is detected for the $B \leftarrow\leftarrow X^1\Sigma^+$ (0, 0), $J' = 4$ transition (see Fig. 6). This corresponds to the smallest spacing between observed rotational energy levels of the B and the $V^1\Sigma^+$ ($v' = 20$) states for equal J' values for $J' = 4$ (see Table I) due to a near-resonance interaction between the two states.[16,20,27] Analysis of the line shifts allowed evaluation of $W_{12} = 2.7$ cm^{-1} ($W'_{12} = 0.6$ cm^{-1}) for $J' = 4$ for $H^{35}Cl$. Good consistency in calculated and experimental values for the ion ratios $I(^{35}Cl^+)/I(H^{35}Cl^+)$ was obtained for $\gamma = 0.002$ and $\alpha = 3.1$ (Fig. 6 and Table II). The B state has been assigned as an $\Omega = 2$ state.[9] The low γ value of 0.002 resembles those observed earlier for triplet states (see above and Ref. 28) which indicates that the B state is a $^3\Delta_2$ state.

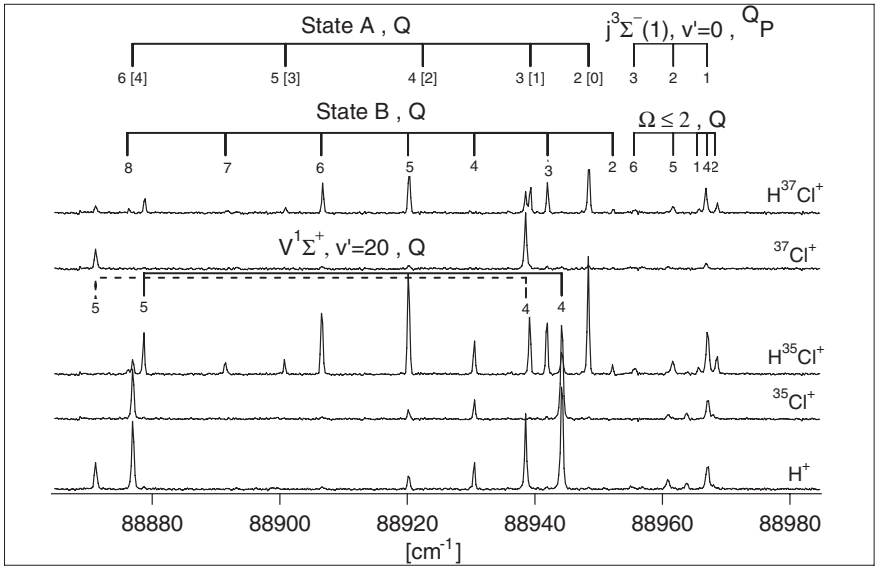

FIG. 5. 1D-$(2+n)$ REMPI spectra for H^+, $^{35}Cl^+$, $H^{35}Cl^+$, $^{37}Cl^+$, and $H^{37}Cl^+$ derived from HCl with isotope ratios in natural abundance for the two-photon excitation region of 88865–88985 cm^{-1}. Assignments for $A \leftarrow\leftarrow X\,^1\Sigma^+$ (0, 0), $B \leftarrow\leftarrow X\,^1\Sigma^+$ (0, 0), $j^3\Sigma^-_1 \leftarrow\leftarrow X^1\Sigma^+$ (0, 0), and $\Omega' \leq 2 \leftarrow\leftarrow X^1\Sigma^+$ (0, 0) spectra ($H^{35}Cl$ and $H^{37}Cl$) are shown. Assignments for $V^1\Sigma^+ \leftarrow\leftarrow X^1\Sigma^+$ (20, 0) are shown for $H^{35}Cl$ as solid lines and for $H^{37}Cl$ as broken lines. Assignments from Ref. 9 for $A \leftarrow\leftarrow X\,^1\Sigma^+$ (0, 0) are in brackets. $J = J'$—numbers are indicated in the figure.

The spectral peaks due to the $A \leftarrow\leftarrow X\,^1\Sigma^+$ (0, 0) transition are marked according to the assignment given by Green *et al.*[9] with numbers inside brackets in Fig. 5. These have been reassigned based on our analysis of the 2D REMPI data, as shown in the figure, for reasons which will now be discussed.

Both the *A* and the *B* spectra show characteristic drops in peak intensities for the parent ions ($H^{35}Cl^+$ and $H^{37}Cl^+$) as J' increases. The intensities for the *B*-spectra, reach minima for the resonance perturbed levels $J' = 4$. As a matter of fact that peak is hardly observable for $H^{37}Cl^+$. Similarly, the *A*-spectra show either no peaks or very weak peaks[9] corresponding to the $J' = 2$ assignment given by Green *et al.* both for $H^{35}Cl$ and $H^{37}Cl$. This is characteristic for near-resonance interactions with the ion-pair state $V(^1\Sigma^+)^{20}$, which in this case must be for $v' = 20$. Both for the *B* and the *A* states the closes rotational levels, in energy, which belong to the $V(v' = 20)$ state are those for $J' = 4$ (see Fig. 5). The spacing, $\Delta E_{J'=4}$, for the *A* state ($H^{35}Cl$) is about 22.0 cm^{-1} (see Table I for the *B* state). It can, therefore, be concluded that the peaks assigned as $J' = 2$ for the *A* spectrum are in fact due to transitions to $J' = 4$ levels. This puts the first peaks in the line series as $J' = 2$, suggesting that the *A* state is an $\Omega = 2$ state. Other peaks in the *A* spectrum are reassigned accordingly in Fig. 5. Furthermore, there are no significant Cl^+ masses detected for any of the rotational transitions in the $A \leftarrow\leftarrow X\,^1\Sigma^+$ (0, 0) system which would be expected if the *A* state was an $\Omega = 0$ state.[27] Whereas the previous assignment gives a low rotational constant , B', of 5.7941 cm^{-1} for the *A* state, which certainly might be expected if it was an $\Omega' = 0$ state,[15,16] our reassignment gives $B' = 9.08$ cm^{-1}, which is typical for a Rydberg state with weak or negligible Rydberg-valence state mixing. Further analysis of the *A* state spectrum, based on the new assignment gives $D' = 0.0185$ cm^{-1} and $\nu^0 = 88957.6$ cm^{-1}. For comparison, $B' = 8.954$ cm^{-1} and $D' = -0.0042539$ cm^{-1} for the *B* state, which has been assigned as an $\Omega' = 2$ state.[9]

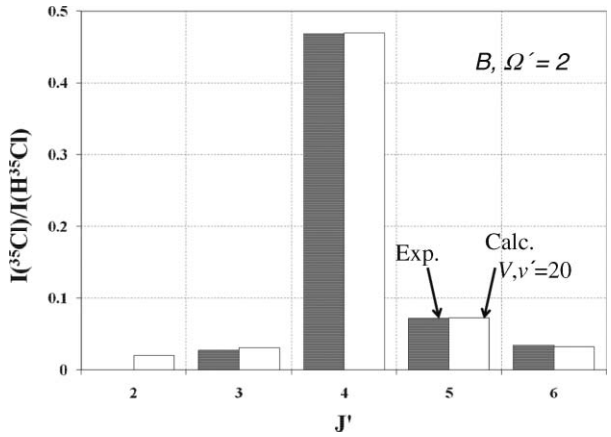

FIG. 6. Relative ion signal intensities, $I(^{35}Cl^+)/I(H^{35}Cl^+)$ vs J' derived from *Q* rotational lines of REMPI spectra due to resonance transitions to the $\Omega' = 2$ (88959.9 cm^{-1}) (*B*) state (gray columns) and simulations, assuming J' level-to-level interactions between the Rydberg state and the $V^1\Sigma^+$ ($v' = 20$) state (white columns).

IV. CONCLUSIONS

Two-dimensional $(2+n)$ REMPI data for HCl, obtained by recording ion mass spectra as a function of the laser frequency, were recorded for the two-photon resonance excitation region 88865– 89285 cm^{-1}. Spectra for $H^{35}Cl$ and $H^{37}Cl$, due to resonance transitions to the ion-pair states $V^1\Sigma^+$ ($v' = 20$, 21) and four Rydberg states, $j^3\Sigma^-(0^+)(v' = 0)$, $j^3\Sigma^-_1(v' = 0)$ and states centered at $= 88957.6$ cm^{-1} (*A*) and 88959.9 cm^{-1} (*B*) for $H^{35}Cl$ were studied. A combined analysis of rotational line shifts and ion signal intensities was performed, developed, and used to derive information relevant to state interactions strengths, photofragmentation

channels, rotational energy characterization, and/or state assignments.

Interaction strengths, W_{12}, and fractional state mixing (c_1^2/c_2^2) due to Rydberg to ion-pair ($V^1\Sigma^+$ ($v' = 20, 21$)) state interactions were evaluated for the Rydberg states $j^3\Sigma^-(0^+)(v' = 0)$, $j^3\Sigma^-{}_1(v' = 0)$ for H^iCl; $i = 35, 37$ and for the B state ($H^{35}Cl$) from rotational line shift analysis. Enhancements in relative Cl^+ ion intensities, $I(^iCl^+)/I(H^iCl^+)$, are observed in all cases for J' levels corresponding to near-resonance interactions. Data for intensity ratios as a function of J' were compared to model expressions which take account of the major ion formation channels following excitations to the Rydberg states, state interactions as well as dissociation channels. The observations for the $j^3\Sigma^-{}_1(v' = 0)$ and the B states could be interpreted as being due to level-to-level interactions between the Rydberg states and the $V(v' = 20)$ states, whereas interactions both with $V(v' = 20$ and 21) needed to be taken account of to explain the observation for the $j^3\Sigma^-(0^+)(v' = 0)$ states. Fit analysis gave parameters which measure the importance of dissociation (predissociation and/or photodissociation) channels in the ionization processes. The weight of dissociation channels are found to be significantly larger for the $\Omega' = 0$ states ($j^3\Sigma^-(0^+)$) than for the $\Omega' = 1, 2$ states which have been studied.

Relative ion signals as a function of J' proved to be useful guide to assigning rotational peak spectra and allowed reassignments of the spectra due to the transitions to the $j^3\Sigma^-(0^+)(v' = 0)$ and the A ($v^0 = 88957.6\ cm^{-1}$) state. The A state was characterized as an $\Omega' = 2$ state with rotational parameters $B' = 9.08\ cm^{-1}$ and $D' = 0.0185\ cm^{-1}$.

ACKNOWLEDGMENTS

The financial support of the University Research Fund, University of Iceland, the Icelandic Science Foundation as well as the Norwegian Research Council is gratefully acknowledged.

[1] W. C. Price, Proc. R. Soc. London, Ser. A **167**, 216 (1938).
[2] S. G. Tilford, M. L. Ginter, and J. T. Vanderslice, J. Mol. Spectrosc. **33**, 505 (1970).
[3] S. G. Tilford and M. L. Ginter, J. Mol. Spectrosc. **40**, 568 (1971).
[4] D. S. Ginter and M. L. Ginter, J. Mol. Spectrosc. **90**, 177 (1981).
[5] J. B. Nee, M. Suto, and L. C. Lee, J. Chem. Phys. **85**, 719 (1986).
[6] T. A. Spiglanin, D. W. Chandler, and D. H. Parker, Chem. Phys. Lett. **137**(5), 414 (1987).
[7] D. S. Green, G. A. Bickel, and S. C. Wallace, J. Mol. Spectrosc. **150**(2), 303 (1991).
[8] D. S. Green, G. A. Bickel, and S. C. Wallace, J. Mol. Spectrosc. **150**(2), 354 (1991).
[9] D. S. Green, G. A. Bickel, and S. C. Wallace, J. Mol. Spectrosc. **150**(2), 388 (1991).
[10] D. S. Green and S. C. Wallace, J. Chem. Phys. **96**(8), 5857 (1992).
[11] E. d. Beer, B. G. Koenders, M. P. Koopmans, and C. A. d. Lange, J. Chem. Soc. Faraday Trans. **86**(11), 2035 (1990).
[12] Y. Xie, P. T. A. Reilly, S. Chilukuri, and R. J. Gordon, J. Chem. Phys. **95**(2), 854 (1991).
[13] Á. Kvaran, H. Wang, and Á. Logadóttir, Recent Res. Dev. Physical Chem. **2**, 233 (1998).
[14] E. d. Beer, W. J. Buma, and C. A. d. Lange, J. Chem. Phys. **99**(5), 3252 (1993).
[15] Á. Kvaran, Á. Logadóttir, and H. Wang, J. Chem. Phys. **109**(14), 5856 (1998).
[16] Á. Kvaran, H. Wang, and Á. Logadóttir, J. Chem. Phys. **112**(24), 10811 (2000).
[17] Á. Kvaran, H. Wang, and B. G. Waage, Can. J. Phys. **79**, 197 (2001).
[18] H. Wang and Á. Kvaran, J. Mol. Struct. **563–564**, 235 (2001).
[19] Á. Kvaran and H. Wang, Mol. Phys. **100**(22), 3513 (2002).
[20] Á. Kvaran and H. Wang, J. Mol. Spectrosc. **228**(1), 143 (2004).
[21] R. Liyanage, R. J. Gordon, and R. W. Field, J. Chem. Phys. **109**(19), 8374 (1998).
[22] M. Bettendorff, S. D. Peyerimhoff, and R. J. Buenker, Chem. Phys. **66**, 261 (1982).
[23] C. Romanescu and H. P. Loock, J. Chem. Phys. **127**(12), 124304 (2007).
[24] C. Romanescu, S. Manzhos, D. Boldovsky, J. Clarke, and H. Loock, J. Chem. Phys. **120**(2), 767 (2004).
[25] A. I. Chichinin, C. Maul, and K. H. Gericke, J. Chem. Phys. **124**(22), 224324 (2006).
[26] A. I. Chichinin, P. S. Shternin, N. Godecke, S. Kauczok, C. Maul, O. S. Vasyutinskii, and K. H. Gericke, J. Chem. Phys. **125**(3), 034310 (2006).
[27] Á. Kvaran, K. Matthíasson, H. Wang, A. Bodi, and E. Jonsson, J. Chem. Phys. **129**(17), 164313 (2008).
[28] A. Kvaran, K. Matthiasson, and H. Wang, J. Chem. Phys. **131**(4), 044324 (2009).
[29] S. Kauczok, C. Maul, A. I. Chichinin, and K.-H. Gericke, J. Chem. Phys. **133**, 024301 (2010).
[30] K. Matthiasson, H. Wang, and A. Kvaran, J. Mol. Spectros. **255**(1), 1 (2009).
[31] Á. Kvaran, K. Matthíasson, and H. Wang, Physical Chemistry; An Indian Journal **1**(1), 11 (2006).
[32] M. H. Alexander, X. N. Li, R. Liyanage, and R. J. Gordon, Chem. Phys. **231**(2–3), 331 (1998).